

# On Fixed-point Iterations for the Solution of Control Equations in Power Systems Transients

C. F. Mugombozi, J. Mahseredjian, O. Saad

**Abstract**—This paper contributes towards the establishment of a formal analysis method of control system equations solved through fixed-point iterations. The success of fixed-point iterations relies on contraction properties of the function to be iterated. A convergence criterion is presented and accuracy is not sacrificed over gain in computational time.

The presented algorithms are illustrated in EMTP-RV for practical control systems used in wind power generation and for a user defined model case. Limitations and performances are discussed in relation to the Newton method.

**Keywords:** Control system equations, fixed-point iterations, Coates graph, feedback interconnection, EMTP.

## I. INTRODUCTION

AN iterative Newton method for the solution of control system equations in Electromagnetic Transient (EMT) type simulation methods has been proposed in [1]. Although such a method is a robust and systematic approach, there are some feedback based control system diagrams that can also be solved using the much simpler and sometimes more efficient fixed-point (FP) method. The efficiency level of the FP method can be very high since it sequentially evaluates the control blocks and does not require time-consuming linearization procedures and matrix formulations required in the Newton method. The difficulty lies on the determination of whether or not the FP method can converge, for a given case, before it is actually undertaken.

Moreover, in some classes of control equations, the model loops may lead to algebraic constraints. In such case, basic sequential evaluation of blocks outputs is not applicable. Different approaches are undertaken to reformulate models in order to apply sequential solution. One approach used in [2] consists in breaking algebraic loops. This is formally acceptable when the loop is artificial, *i.e.* when it can be eliminated without compromising the physical behavior of the model. Specific tools are dedicated to achieve such elimination [3]. However, some cases require algebraic constraints that can not be easily eliminated. A possible

solution consists in re-organizing blocks to eliminate algebraic loops while still maintaining functionality, but as pointed out in [3], this may become prohibitively difficult.

In addition, while such loop-breakings are valid for some classes of control equations, it was proven that they may fail for others, for instance, when certain nonlinear (NL) blocks appear in the feedback path [1]. In fact, loop-breaking may compromise viability or accuracy requirements. A highly accurate algorithm should handle algebraic loops by solving a set of NL simultaneous control equations while, however, increasing the computational time. There is hence a dilemma between lowering accuracy requirements and increasing simulation speed.

It is proposed in this paper to analyze control equations to formally display the contractive properties of loop paths. The success of FP method relies on contraction properties of the function to be iterated [4][5][6][7]. The functions to be iterated were introduced in the formulation of control equations in [8] and specific variables were isolated to fully represent complex looped control systems. It is proposed, in this paper, to study those functions by analyzing the Jacobian matrix in association with isolated variables representing the feedback loop path. Graph theory techniques are used in that purpose. The consideration of such properties may widen the usage of FP methods. When the convergence criterion is established, accuracy is not sacrificed over gain in computation time. Additional iterations permit reaching predefined tolerance.

The analysis proposed in this paper is illustrated for practical control systems in the study of power systems transients, including wind power generation and user defined algebraic equations for an electrical machine model.

This paper contributes to the establishment of a formal analysis method of control system equations which permits a safe use of efficient FP methods.

## II. THEORETICAL BACKGROUND

The literature on theoretical and fundamental aspects related to the FP method is abundant [4]. We will thus restrict our review to the solution of systems of equations of the form:

$$\mathbf{e} = \boldsymbol{\varphi}(\mathbf{e}) \quad (1)$$

where  $\boldsymbol{\varphi}$  is a vector function and  $\mathbf{e}$  is the vector of unknowns. A solution  $\hat{\mathbf{e}}$  of (1) is said to be a FP of  $\boldsymbol{\varphi}$ , since  $\boldsymbol{\varphi}$  leaves  $\hat{\mathbf{e}}$  invariant. The classical approach starts by setting an initial vector  $\mathbf{e}^0$  and computing  $\mathbf{e}^1 = \boldsymbol{\varphi}(\mathbf{e}^0)$  to continue iteratively (iteration counter is  $k$ ) with successive evaluations

---

This work was supported in part by le Fonds Québécois de la Recherche sur la Nature et les Technologies (FQRNT).

C. F. Mugombozi (e-mail: [mugombozi.chuma-francis@ireq.ca](mailto:mugombozi.chuma-francis@ireq.ca), corresponding author) and O. Saad (e-mail: [saad.omar@ireq.ca](mailto:saad.omar@ireq.ca)) are with Hydro-Québec/IREQ, Power systems and Mathematics Unit, 1800 Boulevard Lionel Boulet, Varennes, Québec, J3X 1S1, Canada.

J. Mahseredjian (e-mail: [jeanm@polymtl.ca](mailto:jeanm@polymtl.ca)) is with École Polytechnique de Montréal, 2500 Édouard Mont-Petit, Montreal, H3T 1J4, Canada.

Paper submitted to the International Conference on Power Systems Transients (IPST2013) in Vancouver, Canada July 18-20, 2013.

$\mathbf{e}^{k+1} = \boldsymbol{\varphi}(\mathbf{e}^k)$  until convergence. The contraction mapping theorem gives sufficient conditions under which there is a fixed point  $\hat{\mathbf{e}}$  of (1). It is defined, in general, from mathematical theory [4][5][6]. Formally a vector-valued function  $\boldsymbol{\varphi}$  is a contraction at a point  $\hat{\mathbf{e}}$  if a constant  $\sigma$  exists, with  $0 < \sigma < 1$ , in such a way that:

$$\|\boldsymbol{\varphi}(\mathbf{e}) - \boldsymbol{\varphi}(\hat{\mathbf{e}})\| < \sigma \|\mathbf{e} - \hat{\mathbf{e}}\| \quad (2)$$

for all  $\mathbf{e}$  sufficiently close to  $\hat{\mathbf{e}}$  and where  $\|\cdot\|$  is a specific norm to be defined. In discrete dynamic system simulations we are concerned with here, one focuses specifically on Euclidean space. Also, some assumptions are made including at least, that all elements of  $\boldsymbol{\varphi}$  are piecewise-continuous and, also, that the derivatives of control block functions are well defined and are not infinite. Similar assumptions are made for Newton methods [6],[9].

The following condition of contraction [7] is used in this paper:

$$\|\boldsymbol{\varphi}'(\hat{\mathbf{e}})\|_{\text{spectral}} < 1 \quad (3)$$

where  $\|\cdot\|_{\text{spectral}}$  is the spectral norm and  $\boldsymbol{\varphi}'$  is the Jacobian matrix of  $\boldsymbol{\varphi}$ . The vector-valued  $\boldsymbol{\varphi}$  is a mapping of vector-valued, possibly nonlinear functions, defined through algebraic equations representing a discrete dynamical system. Thus we assume, in EMT-type simulations, a suitable discretization of models (using Trapezoidal rule) at a given time-step, such that all terms including history, inputs and outputs of models can be expressed as (1). In the following section the formulation of  $\boldsymbol{\varphi}$  is recalled from [8].

### III. FIXED-POINT ITERATIONS: FORMULATION AND APPLICATIONS

#### A. Functions on feedback paths

The vector-valued functions on feedback paths that were presented in [8] are recalled here for the presentation of (3). Simultaneous systems of equations can be represented as feedback equations [8]. Basically, a proper cutset is introduced on the graph of control equations in such a way that all cycles are eliminated. The set of variables pertaining to that cutset represent the feedback variables  $\hat{\boldsymbol{\beta}}$  [8]. In other words, the cycles which were removed by cutting each of feedback variables represented by the feedback paths on the graph of the control system. The all-zero eigenvalues condition for the adjacency matrix of the graph can be applied for testing that no cycle remains [10], [11]. This approach provides vector-valued functions  $\mathbf{G}$  and  $\boldsymbol{\varphi}$  for formulating the objective function  $\boldsymbol{\Phi}$  in the application of the Newton method. For a generic case, the system can be represented as

$$\mathbf{e} = \boldsymbol{\varphi}(\mathbf{u}, \mathbf{y}) \quad (4)$$

$$\mathbf{y} = \mathbf{G}(\mathbf{e}) \quad (5)$$

where  $\mathbf{u}$  holds the vector of independent inputs,  $\mathbf{y}$  is found using the application sequence  $\mathbf{G}$  of the control diagram

paths on  $\mathbf{e}$  and the Newton solution is based on:

$$\boldsymbol{\Phi} = \mathbf{e} - \boldsymbol{\varphi}(\mathbf{u}, \mathbf{y}) = \mathbf{0} \quad (6)$$

where  $\mathbf{e}$  holds for feedback variables associated with the cutset  $\hat{\boldsymbol{\beta}}$ .

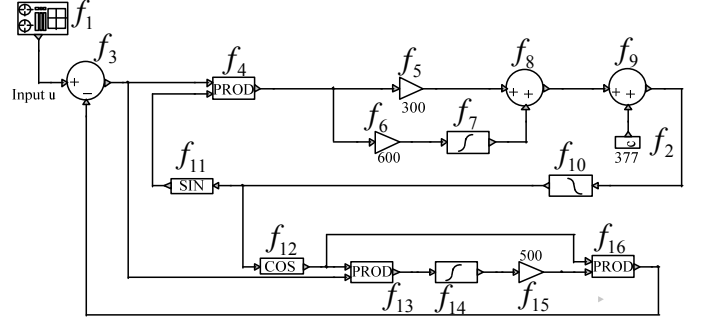


Fig. 1 Phase-locked Loop (PLL) control system from [1]

For illustration purposes, let consider a Phase-Locked Loop (PLL) control studied in [1] and presented in Fig. 1. The process of [8] presented above leads to the set  $\hat{\boldsymbol{\beta}}$  of two feedback functions  $\{f_3, f_4\}$ . The new (reduced) system of equation is consequently given by:

$$e_1 = u - G_1(e_1, e_2) \quad (7)$$

$$e_2 = 0 + G_2(e_1, e_2)$$

where the application sequences (sequential evaluations) are defined by:

$$G_1(\mathbf{e}) = f_{16,15,14,13,12,10,9,8,7,6,5}(\mathbf{e}) \quad (8)$$

$$G_2(\mathbf{e}) = f_{11,10,9,8,7,6,5}(\mathbf{e})$$

and  $\mathbf{e} = [e_1, e_2]$  is the vector of new variables. The FP iterations (FPI) are now defined as:

$$\mathbf{e}^{k+1} = \boldsymbol{\varphi}(\mathbf{G}(\mathbf{e}^k)) \quad (9)$$

Successive FP iterations on (9) will converge for some classes of control systems complying with the contraction mapping theorem recalled in section II. The convergence criterion adopted from [14] is given by:

$$\frac{\|\boldsymbol{\Phi}^k\| - \|\boldsymbol{\Phi}^{k+1}\|}{\|\boldsymbol{\Phi}^k\|} \leq \Phi_{\text{tol}} \quad (10)$$

where  $\Phi_{\text{tol}}$  is a relative tolerance on the objective function and  $\|\cdot\|$  is the Euclidian norm (other equivalent norms may be used). The objective function (6) is rewritten as:

$$\boldsymbol{\Phi}^{k+1} = \mathbf{e}^{k+1} - \boldsymbol{\varphi}(\mathbf{G}(\mathbf{e}^k)) \quad (11)$$

#### B. Application cases

##### 1) Phase-Locked Loop

The method proposed in the previous section is applied to the PLL presented in Fig. 1. The contraction condition is respected for a sufficiently small time-step ( $\Delta t = 1\mu\text{s}$ ) and the found solution is thus comparable to the Newton method solution, using the same  $\Delta t$ . In this case, the FP is clearly disadvantaged, especially when considering that larger time-

steps [1] can be used with the Newton method. Computational performances are summarized in TABLE 1.

TABLE 1 COMPARISON OF SIMULATION TIMES FOR NEWTON AND FP METHODS, PLL CASE

Tolerance relative/absolute	Gain in simulation time FPI vs. Newton
$1e-3/1e-8$	0.96
$1e-4/1e-9$	1.00
$1e-5/1e-10$	1.02

### 2) Simulation of an asynchronous machine

The FP method is applied here for the solution of a user-defined model through control diagram equations for an asynchronous machine model [1]. It comprises 87 blocks including 23 feedback variables. Performances are compared in TABLE 2. Accuracy is assessed in Fig. 2 by comparing the Euclidean norms of relative errors for ten signals. Accuracies of currents at the stator and at the rotor are not acceptable when a single iteration of FP is applied. Setting a fix number of iterations regardless of predefined tolerance is obviously inefficient, since unnecessary iterations may be performed.

It is emphasized that techniques with loop-breaking will not successfully solve this system.

TABLE 2 COMPARISONS OF SIMULATION TIMES FOR NEWTON AND FP METHODS, ASYNCHRONOUS MACHINE MODEL

Tolerance relative/absolute	Time step ( $\mu$ s)	Gain in simulation time FP vs Newton
$1e-4/1e-8$	200	2.02
	400	1.75

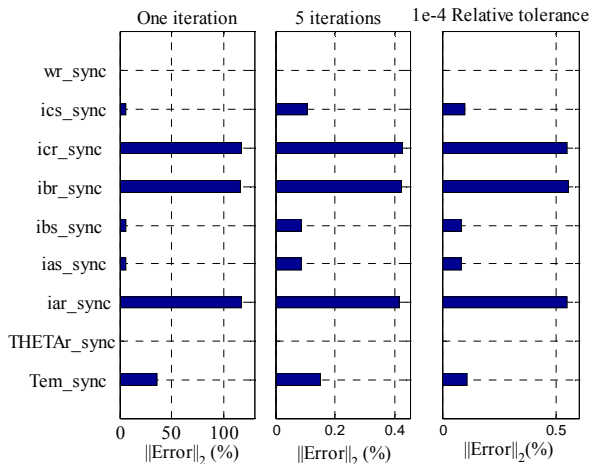


Fig. 2. Euclidean norms of errors, asynchronous machine equations for FP and Newton methods,  $200\mu$ s time-step.

### 3) Wind power plant

The FP method is applied here for the solution of a large scale power system comprising 72 aggregated wind generator models [12] integrated into IEEE-39 bus test system [13]. One of the hundreds of groups of control equations is presented in Fig. 3. The group has one feedback block (see the block SUM with notation FB). Efficiency is presented in TABLE 3. The simulation time-step is  $50\mu$ s for Newton and FP methods.

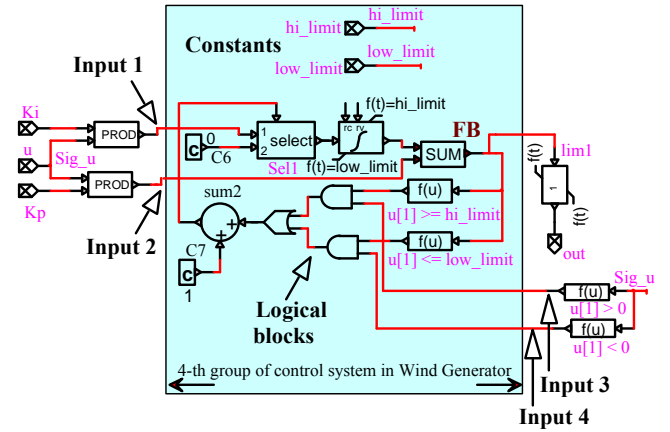


Fig. 3. Sample group of 9 control blocks, 4 inputs and 4 constants, Wind Power generator Model [12], [13].

TABLE 3 SIMULATION TIMES FOR NEWTON AND FP METHODS, LARGE SCALE WIND POWER PLANTS INTEGRATED INTO THE IEEE-39 BUS SYSTEM

Tolerance relative/absolute	Gain in simulation time FPI vs. Newton
$1e-3/1e-8$	1.36

## IV. FORMAL ANALYSIS OF CONTRACTION PROPERTIES

### A. Spectral norms for presented cases

The performance of the FP method is predicted and related to the spectral norm of (3). A larger norm will increase the iteration count in the FP method. If the condition (3) is not respected, the FP method will not converge.

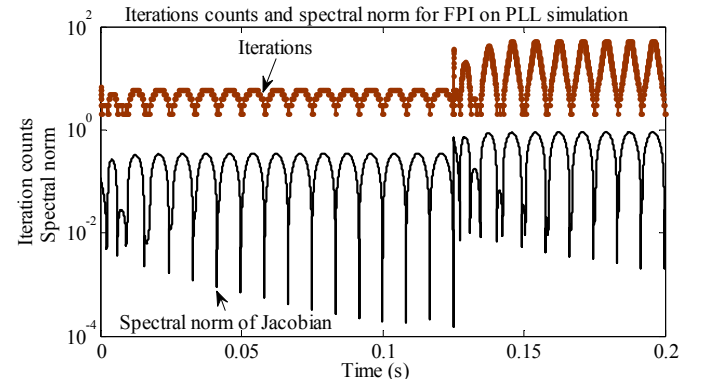


Fig. 4. Spectral norms and iteration counts, PLL case of Fig. 1

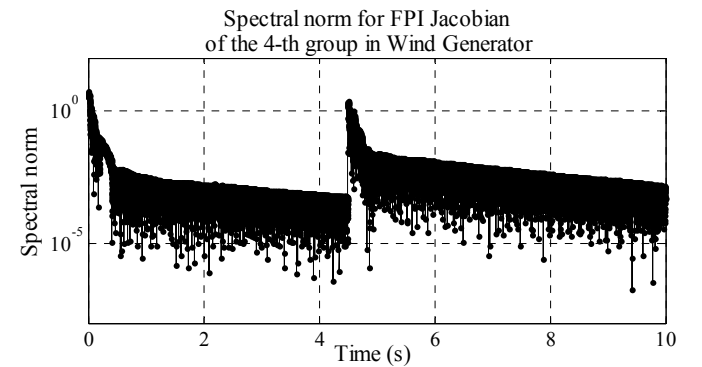


Fig. 5. Spectral norms for Fig. 3

Fig. 4 and Fig. 5 present the spectral norms for the PLL and

wind power plant cases. Fig. 4 uses the feedback variables  $e_1$  and  $e_2$  in Fig. 1. Fig. 5 uses the FB signal shown in Fig. 3. Here, the number of iterations is increased at system initialization and when a fault (short-circuit) is applied in the network.

### B. Estimation of Norm Bounds

The cells of the Jacobian  $\Phi'$  in (3) are partial derivatives of (4) with respect to each feedback variable:

$$J_{ij} = \frac{\partial \varphi_i(\mathbf{u}, G_i(\mathbf{e}))}{\partial e_j} \quad (12)$$

In the discrete time context, numerical perturbation is used for (12). Since  $G_i(\mathbf{e})$  is a composite function on loop path, the loop perturbation concept introduced in [8] can also be used. Equivalently, with care on perturbation values [9],[14], block-by-block perturbation may also be used, as in [1]. In such condition, if  $c_{rs}$  is the partial derivative of the block function  $r$  with respect to input  $s$ , the perturbation value  $\delta_s$  gives the estimated block function derivative:

$$c_{rs} = \frac{\partial}{\partial x_s} f_r \approx \frac{1}{\delta_s} [f_r(\mathbf{x} + [0, \dots, \delta_s, \dots]) - f_r(\mathbf{x})]. \quad (13)$$

The control system can be linearized to represent the Jacobian of the rank corresponding to the count of blocks as in [1]. Such representation is:

$$\delta x_r = \sum_{s=1}^N c_{rs} \delta x_s \quad (14)$$

where  $\delta x_r$  is variable.

A representation of (14) is introduced. The lines (edges) represent partial derivatives and nodes (vertices) represent the variables. For illustration, the Coates graph of the PLL is given in Fig. 6. Similarly the Masson graph [15][16] may also be used, but with slight differences in the definition of equations. Equivalence between both graph representations may be found in [16].

In following lines the goal is the formulation of the topological characteristic of the Jacobian. The term "topological" is used here because the elements in the cells of the Jacobian are linked to the topology of the studied control system. The approach is based on edge-node reduction

techniques on Coates graph [17]. This is also referred to as edges or vertices collapsing in other graph theory literature.

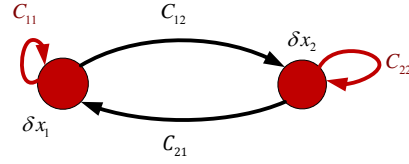


Fig. 7 Coates graph of a system reduced to two variable  $\{x_1, x_2\}$  for feedback path, PLL cases

The approach based on reduction to feedback variables leads to the graph of Fig. 7 for the PLL case shown in Fig. 6. This graph is also the representation of the Jacobian associated to the reduced system in (8). The edges of the graph of the reduced system (see  $C_{ij}$ ) in Fig. 7 are similar to the partial derivative of (8) in the linearized system.

If the system is reduced up to  $M$  variables, the Jacobian of rank  $M$  becomes:

$$\Phi' = [C_{ij}], \quad (15)$$

Where, based on developments from [17]:

$$K(-1)^{-\alpha} C_{ij} = \sum_{\text{grfaX}(gij)}^{\text{per}(\text{Con}(\text{grfaX}(gij)))} (-1)^{\text{LgrfaX}(gij)} \prod \text{grfaX}(gij) \quad (16)$$

where  $K$ ,  $\alpha$  and other terms are defined as in the appendix. The evaluation of (16) for all  $ij$  1-factorial connections and the norm associated to the Jacobian matrix yield the following condition complying with contraction property for 1-norm:

$$\|\Phi'\|_1 = K^{-1} (-1)^\alpha \max_{1 \leq i \leq M} \sqrt{\sum_{j=1}^M C_{ij}} \leq 1 \quad (17)$$

Equation (17) complies with (3). That is the norm bound we propose for formal analysis of contraction properties of the FP method. However, this bound is too complex for estimation in discrete dynamical simulation context. With the manipulation of inequality expressions and using [18], the following upper bounds are proposed:

$$\|\Phi'\|_1 \leq |K^{-1}| \max_{1 \leq i \leq M} \sqrt{\sum_{j=1}^M \max P(i, j) (c_{Max})^N} \quad (18)$$

$$\|\Phi'\|_1 \leq |K^{-1}| \sqrt{M \times (\max(N, (N - M + 2))) \times (c_{Max})^N} \quad (19)$$

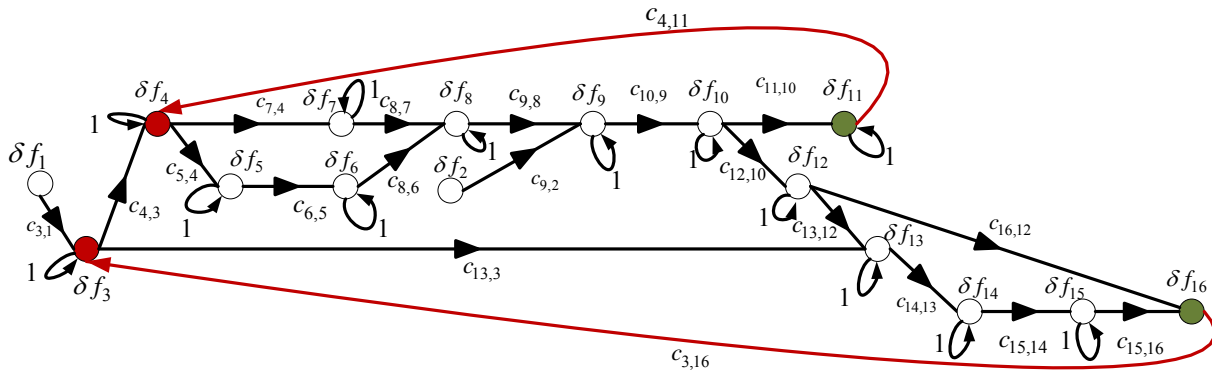


Fig. 6 Coates graph for linearized representation of the PLL in Fig. 1

$$\|\Phi'\|_1 \leq M^2 \prod_j^M C_j \leq M^2 (c_{Max})^M \leq 1 \quad (20)$$

where  $M$  and  $N$  are, respectively, counts of nodes of feedback variables and of all variables,  $K$  is the determinant of graph of nodes which are not feedback variables,  $c_{Max}$  is the maximum partial derivative in the control system and  $\max P(i, j)$  is the maximum of the permanent of connectivity matrix of graph  $g_{ij}$  (see appendix).

### C. Time-delay blocks in loop paths

When there exist time delays in loop paths, FP iterations are “stationary”. The exact solution is found in a single iteration. Such condition is comparable to the loop-breaking mentioned earlier, which satisfies the contraction mapping theorem in (2) with any  $0 \leq \sigma < 1$  and any  $k \geq 1$ . However the breaks which will ensure such “form of delay” within the loop path should be applied on all feedback outputs. Or, at least, in such a way that all cycles will be “delayed”. Formally, with the graph representation, if the vertices associated to the location of delays are virtually cut, all eigenvalues should be zero in the adjacency matrix resulting from the cuts. On the contrary, if any cycle remains, there will subsist at least one non-zero eigenvalue. In general, with no time-delay blocks, the FP solution with single iteration may not converge. See, for example, the errors in Fig. 2.

### D. Linear and bounded derivatives control equations

Some classes of control system equations comprise only linear blocks. The Jacobian matrix is bounded taking into account the highest derivative of blocks which are constants for such linear system. For the simple case in Fig. 8, (15) and (16) yield:

$$\|\Phi'\| = \text{prod}([|c_1|, |c_2|, \dots, |c_5|]) \leq \|c_{Max}\|^5, \quad (21)$$

where  $c_{Max} = \max[|c_1|, |c_2|, \dots, |c_5|]$  is the highest absolute value of block derivatives.

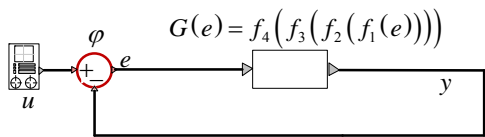


Fig. 8 Simple case of one feedback path reduced from Fig. 10

For illustration purposes, the contraction conditions are compared for the system in Fig. 8. Let assume that the derivatives of block functions are  $[c_j] = [0.7, 0.5, 0.4, c_{Max}]$ , where  $K = 1$  is the determinant of the graph in Fig. 13. The upper bounds of the Jacobian norms are presented in TABLE 4 for the case of Fig. 8. The maximum count of iterations is 100.

For this simple case, it is clear that (21) is below one for all  $|c_{Max}| < 1$ . For  $c_{Max} = 0.75$ , for example, the norm bound condition (3) is respected. The FP iterations will successfully converge. Indeed, within a maximum of 13 iterations, all time

points were solved as presented in Fig. 9. For other values of  $c_{Max}$ , the analysis shows that, up to around 7.1, condition (3) is respected. However, as presented in TABLE 4, for greater values, the spectral norm is higher than one and the FP iterations do not converge. The input signal  $u$  is a sinusoidal input and time step is  $200\mu\text{s}$ .

TABLE 4 COMPARISON OF UPPER BOUND ESTIMATIONS

$c_{Max}$	0.75	25	50
Jacobian norm	0.105	3.5	7.0
Eq. (21)	0.27	9.76e6	3.12e8
Eq. (17)	0.49	3.12e3	1.67e4
Eq. (18)	0.49	3.12e3	1.67e4
Eq. (19)	11.9	7.65e4	4.33e5
Eq. (20)	0.273	9.76e6	3.12e8

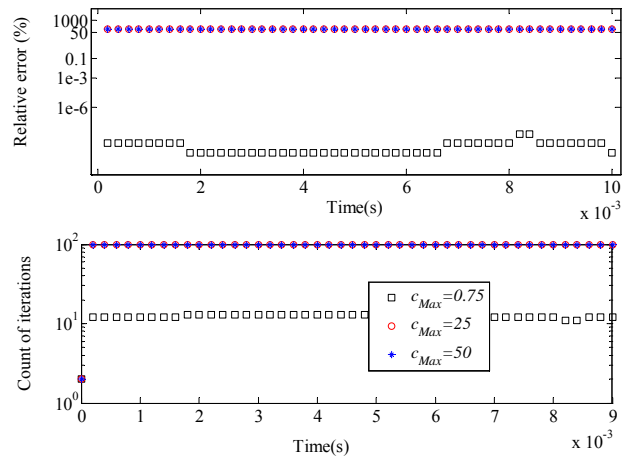


Fig. 9 Illustration of FP iterations on different bounds of derivatives for linear cases: error are against analytic solution of Fig. 8.

It is obvious however that some limiting cases appear for higher disparities between derivatives of blocks. The conservative conditions of contraction may fail while more accurate conditions may succeed, see for instance the bound (19) in TABLE 4. Also, if  $c_{Max}$  is slightly greater than one, (21) will also failed while (3) will not.

Similar analysis may be applied on a more general case including NL blocks, with bounded limits of derivatives and multiple feedback variables.

## V. CONCLUSIONS

This paper contributes towards formal analysis of fixed-point (FP) iterations applied in the context of discrete dynamical simulation. Feedback paths on which iterations are applied were displayed and their contractive properties were analyzed. The FP iterations was applied to practical control equations in the simulation of electromagnetic transients. As the convergence of FP iterations is difficult to predict before it has been undertaken, some contractive bound limits were proposed but are limited to few classes of control systems.

## VI. APPENDIX

A formal representation of the reduction of the graph of control equations to feedback variables uses operations on

Coates graph [17]. The process is illustrated below.

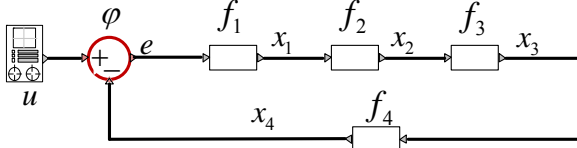


Fig. 10. Simple case for reduction of control equations to only FB variable

The simple system in Fig. 10 has one feedback. Corresponding Coates graph before reduction and after reduction of nodes are respectively presented in Fig. 11 and Fig. 12.

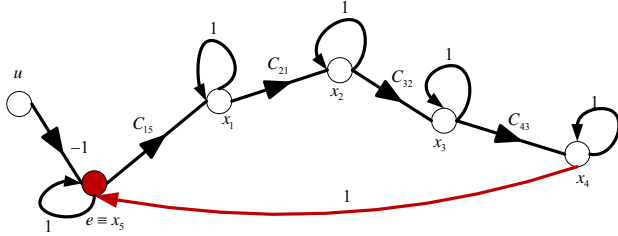


Fig. 11. Coates graph of simple case in Fig. 10 for all linear blocks and single identified FB variable

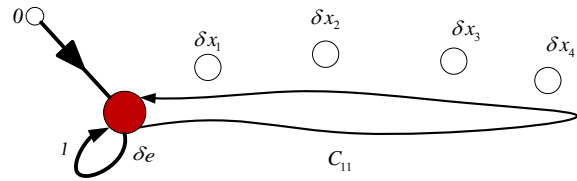


Fig. 12. Coates graph of reduction simple case in Fig. 10 for linearized equations:  $\mathbf{gr}(M)$

In the reduced system representation of equations, the Jacobian associated to the objective function is  $\varphi' = C_{11}$ , where  $C_{11} = c_1 c_2 c_3 c_4 c_5$  is the branch gain in the reduced system, and  $c_r$  is the gain for  $r$ -th linear block or partial derivative of output of  $r$ -th block with respect to the single input. For multiple input blocks, corresponding notation is  $c_{rs}$  as in (13). In general, branch gains are of the following form [17] (page 156):

$$C_{ij} = \frac{(-1)^\alpha}{K} \times \sum_{\mathbf{grfaX}(gij)} \left\{ \frac{(-1)^{L\mathbf{grfaX}(gij)} \times \prod \mathbf{grfaX}(gij)}{\prod \mathbf{grfaX}(gij)} \right\} \quad (22)$$

where:

-  $K$  is the determinant of the sectional graph  $\mathbf{gr}(N-M)$ , such as in Fig. 13;

-  $\mathbf{grfaX}(gij)$  : 1-factorial connection from node  $i$  to node  $j$  in the sectional graph  $gij$ ;

-  $gij$  : graph of eliminated nodes  $\{N-M\}$ , see in Fig. 13, combined to a pair of  $\{i, j\}$  nodes of the new reduced system;

-  $\alpha$  : count of nodes in the graph  $gij$ ;

-  $L\mathbf{grfaX}(gij)$  : count of loops in the graph  $gij$ ;

-  $\prod \mathbf{grfaX}(gij)$  : Product of gains (or partial derivatives) of branches on sectional graph  $\mathbf{grfaX}(gij)$ , i.e.  $c_1 c_2 \dots c_v \dots c_{N_i}$ ;

-  $\text{per}(\text{Con}(\mathbf{grfaX}(gij)))$  : permanent of the matrix of connectivity of the graph  $\mathbf{grfaX}(gij)$ . The  $i$ -th row and the  $j$ -th column of the connectivity matrix are eliminated.

The Jacobian is given by

$$\varphi' = [C_{ij}] \quad (23)$$

Where  $C_{ij}$  is the branch partial derivative between two nodes in the reduced system evaluated as (22).

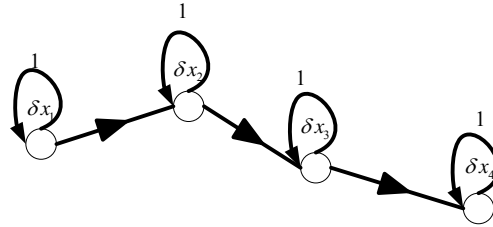


Fig. 13. Sectional graph  $\mathbf{gr}(N-M)$  of eliminated nodes (not FB variables)

## VII. REFERENCES

- [1] J. Mahseredjian, L. Dubé, Ming Zhou, S. Dennetière, G. Joos, "Simultaneous solution of control system equations in EMTP", *IEEE Transactions on Power Systems*, Vol. 21, No. 1, Feb. 2006.
- [2] Matlab/Simulink The MathWorks Inc, *Software Package for Modeling and Analyzing Dynamic Systems*. Simulink [Available online]
- [3] P. J. Mosterman, J. E. Cioffi "Automated approach to resolving artificial algebraic loops", (MathWorks) US Patent 7 167 817 B2, Jan. 23, 2007.
- [4] *Journal of fixed points and applications*, [Online]. Available, Oct. 15 2012: <http://www.fixedpointtheoryandapplications.com/>
- [5] H. K. Khalil, *Nonlinear systems*, Third edition, Prentice hall, 2002.
- [6] J. M. Ortega, W.C. Rheinboldt, *Iterative solution of nonlinear equations in several variables*, Ed. Philadelphia, Pa.: Society for Industrial and Applied Mathematics, 2000
- [7] P. J. Olver, "Numerical solution of algebraic systems", in *AIMS Lecture Notes on Numerical Analysis*, 2006
- [8] C. F. Mugombozi, J. Mahseredjian, O. Saad, "Efficient computation of feedback-based control system equations for electromagnetic transients," *IEEE transactions on Power delivery*, to be published.
- [9] J. E. Dennis, "On the convergence of Newton-like Methods", in P. Rabinowitz (ed.), *Numerical Methods for Nonlinear Algebraic Equations*, Gordon and Breach Science Publishers, 1970.
- [10] B. D. McKay, F. E. Oggie, G. F. Royle, N. J. A. Sloane, I. M. Wanless, H. S. Wilf, "Acyclic Digraphs and Eigenvalues of (0; 1)-Matrices," in *Journal of Integer Sequences*, Vol. 7 (2004).
- [11] D. M. Cvetkovic, M. Doob and H. Sachs, *Spectra of Graphs*, third ed., Barth, Heidelberg, 1995.
- [12] R. Gagnon, G. Turmel, C. Larose, J. Brochu, G. Sybille, M. Fecteau, "Large-Scale Real-Time Simulation of Wind Power Plants into Hydro-Québec Power System", Presented at the 9th International Workshop on Large-Scale Integration of Wind Power into Power Systems as well as on Transmission Networks for Offshore Wind Power Plants, October 18-19 2010, Quebec-city, Québec, Canada.
- [13] C. F. Mugombozi, O. Saad, T. Roudier, V. Morissette, R. Gagnon, G. Sybille, "EMTP- MATLAB/SPS Co-Simulation Applied for Large-Scaled Wind Power Plants", International Council on Large Electric Systems (CIGRE) Canada Conference, Montréal, September 2012.
- [14] J. J. More, G. S. Burton, K. Hillstrom, *User guide for MINPACK-1*, Argonne National Labs Report ANL-80-74, Argonne, Illinois, 1980.
- [15] E. J. Henley, R.A. Williams, *Graph theory in modern engineering*, Academic Press, 1973.
- [16] C. A. Desoer, "The Optimum Formula for the Gain of a Flow Graph or a Simple Derivation of Coates Formula", in Proceedings of the IRE, 1959.
- [17] W. K. Chen *Applied graph theory*, American Elsevier, 1971.
- [18] H. Forbert and D. Marx, "Calculation of the permanent of a sparse positive matrix", *Computer Physics Communications* 150 (2003), 267–273.